



Simulation of a magnetocaloric heating network

Filonenko, Konstantin; Johra, Hicham; Dallolio, Stefano; Engelbrecht, Kurt; Heiselberg, Per Kvals; Bahl, Christian; Veje, Christian T.

Published in:

Thermag 2018, Proceedings of the International Conference on Caloric Cooling

DOI (link to publication from Publisher):

[10.18462/iir.thermag.2018.0001](https://doi.org/10.18462/iir.thermag.2018.0001)

Publication date:

2018

Document Version

Publisher's PDF, also known as Version of record

[Link to publication from Aalborg University](#)

Citation for published version (APA):

Filonenko, K., Johra, H., Dallolio, S., Engelbrecht, K., Heiselberg, P. K., Bahl, C., & Veje, C. T. (2018). Simulation of a magnetocaloric heating network. In *Thermag 2018, Proceedings of the International Conference on Caloric Cooling* (pp. 15-20). Technische Universität Darmstadt.
<https://doi.org/10.18462/iir.thermag.2018.0001>

General rights

Copyright and moral rights for the publications made accessible in the public portal are retained by the authors and/or other copyright owners and it is a condition of accessing publications that users recognise and abide by the legal requirements associated with these rights.

- Users may download and print one copy of any publication from the public portal for the purpose of private study or research.
- You may not further distribute the material or use it for any profit-making activity or commercial gain
- You may freely distribute the URL identifying the publication in the public portal -

Take down policy

If you believe that this document breaches copyright please contact us at vbn@aub.aau.dk providing details, and we will remove access to the work immediately and investigate your claim.

PAPER ID: 0001

DOI: 10.18462/iir.thermag.2018.0001

Simulation of a magnetocaloric heating network**Konstantin FILONENKO^(a), Hicham JOHRA^(b), Stefano DALL'OLIO^(c), Kurt ENGELBRECHT^(c), Per HEISELBERG^(b), Christian BAH^(c), Christian VEJE^(a)**^(a)University of Southern Denmark, Center for Energy Informatics Odense M, DK-5230, Denmark,

[kfi, veje]@mmmi.sdu.dk

^(b)Aalborg University, Division of Architectural Engineering, Department of Civil Engineering Aalborg -st, DK-9220, Denmark, [hj, ph]@civil.aau.dk^(c)Technical University of Denmark, Department of Energy Conversion and Storage, Roskilde, DK-4000, Denmark, [chrb, kuen]@dtu.dk**ABSTRACT**

The concept and methodology of a magnetocaloric heating network is proposed. A small thermal network consisting of several magnetocaloric heat pumps (MCHP) is considered from the point of their scaling and connection properties. We found a linear scaling law following the heating power variation with AMR mass, which can be included in an MCHP lookup table produced by a 1D transient AMR model. To estimate the performance of networks with different number of MCHPs, a set of single MCHPs coupled through temperature boundary conditions are modelled and network formulas are applied for the reference case of Gd packed beds. A performance optimum is found for specific design points compliant with building heating applications.

Keywords: Heating Network, Magnetocaloric Network, Magnetocaloric Heat Pump, Scaling, Cascading, Energy Efficiency, Heating power, Heat Pump Capacity

1. INTRODUCTION

Increasing maturity of magnetocaloric refrigeration technology raises an ambition to employ it in heating applications previously served by vapour compression heat pumps (VCHP). One of the aims of establishing the EnovHeat project was to develop, build and test an MCHP prototype. It was previously numerically demonstrated that an MCHP can be successfully implemented in a low-energy residential house (Johra et al., 2017). However, issues arise with experimental implementation of the proposed system, one of them being the low displaced supply volume per operation cycle. This appears as an insufficient temperature difference across the heat emitter and domination of pump losses over the supplied heating power preventing maximum device performance. The solution proposed here lies in building a magnetocaloric heating network, which is somewhat analogous to conventional VCHP cascading (Tahavori et al., 2017). Due to scalability and modularity of an active magnetic regenerator (AMR), these networks are anticipated to provide an enhanced structural flexibility compared to VCHP and increase the temperature differences compared to a single MCHPs.

Under magnetocaloric network we understand either a single MCHP, which is normally a network of AMRs connected in parallel, or multiple MCHPs connected in any possible way. To apply MCHPs in residential or industrial heating, one has to scale them up. The relation between the sets of scaled and non-scaled values should be given by some mass-scaling law, which is known only for some simple connection types constrained to small temperature differences across the load. The more general scaling law would depend on the precise way the AMR mass is altered, e.g. whether the porosity, hydraulic diameter, aspect ratio and many other parameters of a magnetocaloric material are changed while scaling. Hence, the three important aspects to consider in modeling and comparison of the MCHPs networks are individual AMR properties, their scaling and their dependence on interconnections within the network. Individual properties were studied in detail in various AMR configurations (Lei et al., 2017), therefore, this study focuses on AMR scaling and connections. It proposes a way to generate mass scaling laws and use them in building energy models in form of a lookup table. Given the design point with heating power of 2 kW and COP of 5 suitable for building heating applications, the properties of a scaled and reconnected network are calculated for the reference case of Gd packed bed.

2. MAIN SECTION

2.1. Network Methodology

2.1.1. Scaling types

It is useful to start by looking at MCHP prototype (Engelbrecht et al., 2012), as a special type of an AMR network, which can be constructed by connecting in parallel N_{AMR} identical AMRs, each of magnetocaloric mass m_{AMR} . The total magnetocaloric mass of the network can then be found as $m_{HP} = N_{AMR} m_{AMR}$. Since the mass of the network scales with number of AMRs, the construction of such network will be called *number scaling*. The case with $N_{AMR}=3$ is illustrated in Fig. 1(a), where the network consists of three AMRs (black squares) connected to a common heat source (blue circle) and a common heat load (red circle). If the losses between each pair of AMRs are neglected, the heating power of the network $Q_{H,HP}$ is equal to the sum of individual AMR heating powers, $Q_{H,AMR1}, Q_{H,AMR2}, \dots, Q_{H,AMRN}$. Since number-scaled AMRs are identical, a single AMR heating power $Q_{H,AMR}$ is simply multiplied by N_{AMR} : $Q_{H,HP} = N_{AMR} Q_{H,AMR}$. Since the same is valid for MCHP capacity $Q_{C,HP} = N_{AMR} Q_{C,AMR}$, the COP of the number-scaled network is derived analytically from the single AMR performance: $COP_{HP} = Q_{H,HP} / (Q_{H,HP} - Q_{C,HP})^{-1} = Q_{H,AMR} / (Q_{H,AMR} - Q_{C,AMR})^{-1} = COP_{AMR}$

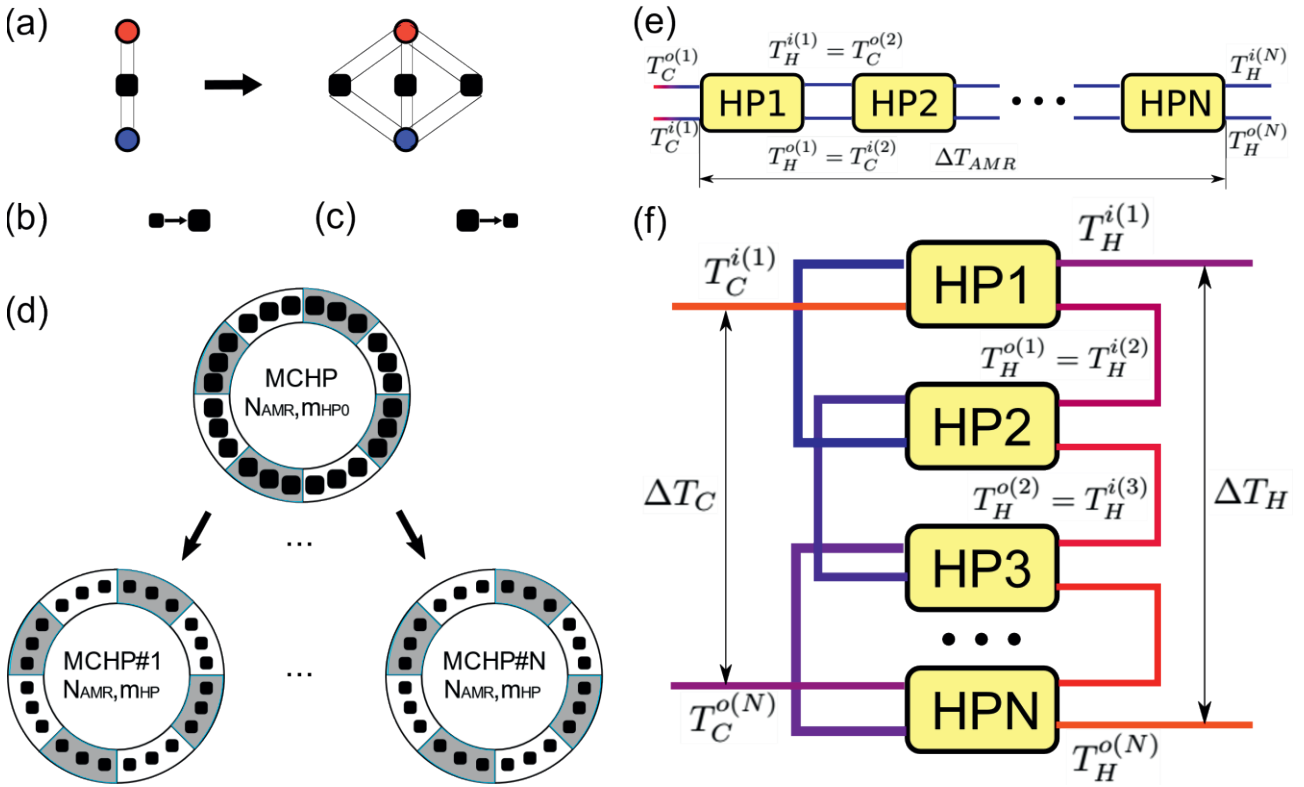


Figure 1: Schematic representation of (a) number scaling ($N=3$) with parallel connection, (b) mass upscaling ($M>1$), (c) mass downscaling ($M<1$), (d) mixed scaling, (e) series connection and (f) cascading. Black squares represent AMRs and their sizes are proportional to AMR masses

Another way to change Q_H is to change the mass of each AMR, while keeping the number of AMRs fixed, $N_{AMR} = const$. The change of the AMR mass proportionally to some scaling factor M will be called *mass scaling*. Mass upscaling (downscaling) are illustrated in Fig. 1(b) (Fig. 1(c)), where the final AMR mass m_{AMR} is greater (less) than its initial mass m_{AMR0} . Mass scaling is thus given by the proportionality relation $m_{AMR} = M m_{AMR0}$ with $M>1$ for upscaling and $M<1$ for downscaling. It is not known *a priori*, in contrast to number scaling, how the heating power of the scaled AMR $Q_{H,AMR}$ depends on the initial heating power $Q_{H,AMR0}$, because the value of the former depends on the way, in which the mass is changed. As a result, the MCHP heating power $Q_{H,HP} = N_{AMR} Q_{H,AMR}$ with total mass $m_{HP} = N_{AMR} m_{AMR} = N_{AMR} M m_{AMR0} = M m_{HP0}$ is also not known from its initial heating power $Q_{H,HP0} = N_{AMR} Q_{H,AMR0}$. To find connection between $Q_{H,HP}$ and $Q_{H,HP0}$, the mass scaling law $Q_{H,HP}(m_{HP})$ must be calculated numerically.

Even less obvious, what will happen if both *number scaling* and *mass scaling* are applied at the same time. The corresponding network configuration is illustrated in Fig. 1(d). The geometry in the figure is used to calculate results in Sec. 2.2.2, therefore, the network description is given in the following points:

1. MCHP prototype with $N_{AMR}=24$ AMRs (Engelbrecht et al., 2012) and total magnetocaloric mass $m_{HPO}=N_{AMR}m_{AMR0}$ is established by number scaling of a single AMR with mass m_{AMR0}
2. Each of the AMRs in the MCHP is number-scaled again to produce N_{HP} identical MCHPs in place of the original MCHP, so that the total mass of the network becomes $m_{net0}=N_{HP}m_{HPO}=N_{HP}N_{AMR}m_{AMR0}$
3. Each AMR in each of the N_{HP} MCHP is mass-downscaled with $M=N_{HP}^{-1}$, so that the new AMR mass is $m_{AMR}=N_{HP}^{-1}m_{AMR0}$ and the network mass is now $m_{net}=N_{HP}^{-1}N_{HP}m_{HPO}=m_{HPO}$

Point 3 is important for comparison between the network and single MCHP performances, in which case one must have the total network mass equal to that of a single MCHP.

2.1.2. Connection types

The network number-scaled from a single AMR in previous section, further called *parallel network*, connects AMRs to a common heat source on their cold side and to a common heat sink on their hot side. AMRs are independent in the sense they are not connected to each other and, therefore, the network capacity $Q_{C,net}$, heating power $Q_{H,net}$ and COP can be calculated analytically from a single AMR performance:

$$Q_{C,H},net = N_{HP}Q_{H,HP} = N_{HP}N_{AMR}Q_{C,H},AMR \quad \text{Eq. (1)}$$

$$COP_{net} = Q_{H,net} (Q_{H,net} - Q_{C,net})^{-1} = Q_{H,AMR} (Q_{H,AMR} - Q_{C,AMR})^{-1} = COP_{AMR} \quad \text{Eq. (2)}$$

We will consider another well-known type of connection, a *series network*, where the hot outlet at temperature $T^{o(n)}_H$ (hot inlet at temperature $T^{i(n)}_H$) of MCHPⁿ, is connected to the cold inlet at $T^{i(n+1)}_C$ (cold outlet at $T^{i(n+1)}_C$) of MCHP⁽ⁿ⁺¹⁾ as shown in Fig. 1(e), where $n = 1:N_{HP}$. This topology leads to heat transfer between MCHPs, described by additional terms in the energy balance Eq. (1). Since $T^{i(n)}_H < T^{i(n+1)}_H$, the temperature difference $\Delta T_{AMR} = T^{i(N)}_H - T^{i(1)}_C$ between the hot and cold inlets to the network increases with each added MCHP. However, the heat transferred to and from the heat transfer fluid per cycle, $Q_{C,net} \Delta V_C \Delta T_C$ and $Q_{H,net} \Delta V_H \Delta T_H$, depends only on its displaced volume and temperature difference in MCHP¹ (V_C and $\Delta T_C = T^{i(1)}_C - T^{o(1)}_C$) and MCHP^N (V_H and $\Delta T_H = T^{o(N)}_H - T^{i(N)}_H$). The volumes V_C and V_H displaced during the hot and cold blow do not depend on N_{HP} , and, therefore, the heating power magnitude is primarily defined by the value of ΔT_H for changing N_{HP} . As our simulations show, ΔT_H cannot be made large enough to compensate for pump losses in the whole range of temperatures used by residential heating systems. The same applies to parallel networks.

The need for larger ΔT_H made the authors search and simulate the network connection referred to as *cascading* (Tahavori et al., 2017), with its topology shown in Fig. 1(f). Cascading can be classified as a series connection, because it uses the same principle of connecting outlet of MCHPⁿ with inlet of MCHP⁽ⁿ⁺¹⁾. However, MCHP connections are hot-to-hot and cold-to-cold and not hot-to-cold and cold-to-hot: hot outlet at temperature $T^{o(n)}_H$ (cold outlet at temperature $T^{o(n)}_C$) of MCHPⁿ is connected to the hot inlet at $T^{i(n+1)}_H$ (cold inlet at $T^{i(n+1)}_C$) of another MCHP⁽ⁿ⁺¹⁾ as shown in Fig. 1(e). As a result, no heat transfer exists between MCHPs, so that the capacities and heating powers can be summed directly, e.g.

$$Q_{H,net} = \sum Q_{Hn,HP}(m_{HP}) = N_{AMR} (Q_{H1,AMR} + Q_{H2,AMR} + \dots + Q_{HN,AMR}) \quad \text{Eq. (3)}$$

If $T^{i(n)}_H < T^{i(n+1)}_H$, which should be the case for normal heat pump operation, the temperature difference $\Delta T_H = T^{i(N)}_H - T^{i(1)}_H$ between the hot outlet and inlet of the network must increase with each added MCHP. This is expected to lead to an increase in either heating power, when COP_{net} is fixed, or in COP_{net} when $Q_{H,net}$ is fixed. This hypothesis was checked by (Tahavori et al., 2017) only for the case with $N_{HP}=3$ and fixed COP, but the study was never brought further to check for another N_{HP} or fixed heating power.

2.2. Numerical results and discussion

Based on scaling laws one can create fast and accurate energy models of magnetocaloric networks using precalculated 5D lookup tables (Johra et al., 2018). The first aim of this section is to find a way for mass-scaling laws $Q_{H,HP}(m_{HP})$ and $Q_{C,HP}(m_{HP})$ to be tabulated from simulations. The second aim is to calculate the performance of cascaded networks to see how they can improve MCHP heat transfer or performance. The magnetocaloric packed sphere bed parameters listed in Table 1 are used in the 1D model of AMR (Engelbrecht, 2008) to produce all results presented in this section.

Table 1. Packed sphere AMR parameters

N_{AMR}	m_{AMR0} , kg	L , m	A , cm ²	ρ , kg m ⁻³	ϵ	d , mm	T_{Curie} , K	τ , s	V_H , L hr ⁻¹
24	0.117	$0.1 M^{1/3}$	$2.2925 M^{2/3}$	7900	0.36	0.6	292	2	$200\tau N_{AMR}^{-1} N_{HP}^{-1}$

2.2.1. Scaling

MCHP capacity $Q_{C,HP} = N_{AMR} Q_{C,AMR}$, its heating power $Q_{H,HP} = N_{AMR} Q_{H,AMR}$ and COP are calculated and plotted in Fig. 2 for mass- and number- scaled AMRs. Mass scaling is performed by changing AMR length L and its cross-section A keeping all other parameters fixed (see Tahavori et al., 2017). The AMR model is solved for several mass values $m_{AMR} = M_i m_{AMR0}$ with $M_i = 0.25 (2i - 1)$ and $i=1:14$. Corresponding values of $Q_{C,HP}(m_{HP})$, $Q_{H,HP}(m_{HP})$ and COP(m_{HP}) are shown as empty circles and their quadratic and linear fits are shown as solid and dashed lines, respectively. As a result, the heat transfer rates are given either as $Q_{C,HP} = 51.48 m_{HP} - 4.297 [W]$ and $Q_{H,HP} = 64.06 m_{HP} - 19.84 [W]$ or $Q_C = -0.1082 m_{HP}^2 - 53.59 m_{HP} - 11.15 [W]$ and $Q_H = 0.1287 m_{HP}^2 + 61.55 m_{HP} - 11.68 [W]$ and the corresponding COPs are post-calculated from Q_C and Q_H . To compare the two types of scaling, $N_{AMR} M_i = 6$ out of 24 AMRs are taken as reference MCHP and each of them is number-scaled so that the resulting parallel network can be described by relations $m_{net0} = 6 N_{HP} m_{AMR0}$, $Q_{C,net} = 6 N_{HP} Q_{C,AMR0}$ and $Q_{H,net} = 6 N_{HP} Q_{H,AMR0}$. The values of $Q_{C,net}$, $Q_{H,net}$ and COP_{net} corresponding to $N_{HP} = 1:27$ are plotted as solid circles.

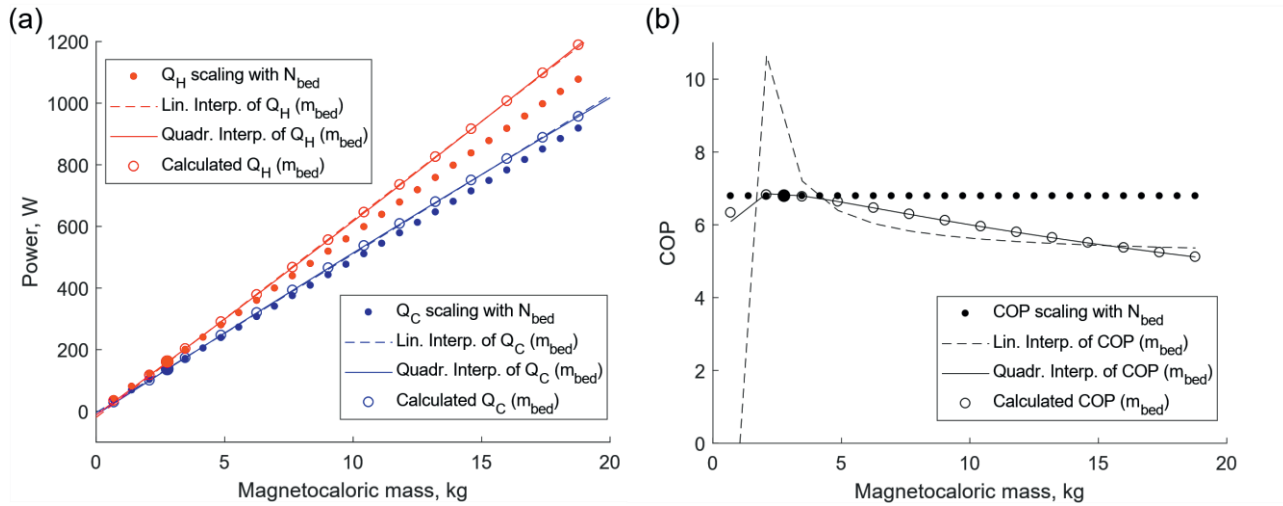


Figure 2: Mass- and number- scaling laws for (a) heating power, capacity and (b) COP

As can be observed, both quadratic and linear mass-scaling laws accurately approximate Q_C and Q_H values. However, the linear approximation for COP is inaccurate, which makes quadratic fit the only possibility for scaling law to be integrated into an AMR lookup table, which requires 2 additional elements to be added to the 5th dimension of the lookup table. The third polynomial coefficient can be post-calculated, since the reference values for $Q_{C,HP0}$ and $Q_{H,HP0}$ are already contained in the same dimension. As for the parallel network values (solid circles), it is found that the power values are reduced compared to mass-scaled network, but the COP stays larger in the whole range.

2.2.2. Cascading

To check the hypothesis, that cascading improves either heating power or COP, the network configuration in Fig. 1(d) is chosen. Cold-to-cold and hot-to-hot series connections are established between separate heat pumps $MCHP^1, MCHP^2, \dots MCHP^{N_{HP}}$, as explained in Fig. 1(e). Calculations are made for seven different networks with $N_{HP} = 1-7$, where $N_{HP} = 1$ corresponds to the reference case of a single heat pump with no mass scaling. For each fixed N_{HP} , the outlet temperatures of $MCHP^1$, $T^{(2)}_C$ and $T^{(2)}_H$, and its heating power $N_{AMR} Q_{H1,AMR}$ are calculated from a 1D model based on the fixed inlet temperatures $T^{(1)}_C = 282.15$ K and $T^{(1)}_H = 302.15$ K as boundary conditions. Using $T^{(2)}_C$ and $T^{(2)}_H$ as inlet boundary conditions, the outlet temperatures for $MCHP^2$, $T^{(3)}_C$ and $T^{(3)}_H$, and its heating power $N_{AMR} Q_{H2,AMR}$ are found. Repeating this procedure for all $MCHP$ in the network, the outlet temperatures of $MCHP^{N_{HP}}$, $T^{(N)}_C$ and $T^{(N)}_H$, and its heating power $N_{AMR} Q_{HN,AMR}$ are calculated. The total heating power of the network is then found from Eq. (3) and the mass flow rate is calculated as $m_{flow} = Q_{H,net} c_f^{-1} \Delta T_H^{-1}$. Fig. 3 shows COP_{net} , m_{flow} and temperature gain ΔT_H optimized to fit the target $Q_{H,net} = 2$ kW, which is chosen as typical heating demand in a typical single family house. It is confirmed in Fig. 3(a) for different N_{HP} that the network supplies more heat to the system, than a single $MCHP$, for the same total magnetocaloric mass and the same system COP and the optimum number of heat pumps in the network equal to $N_{HP} = 3$. Figs. 3(b) and 3(c) show that m_{flow} in the system reduces rapidly and ΔT_H increases with increasing N_{HP} , which means larger heating power of the heating system per displaced volume.

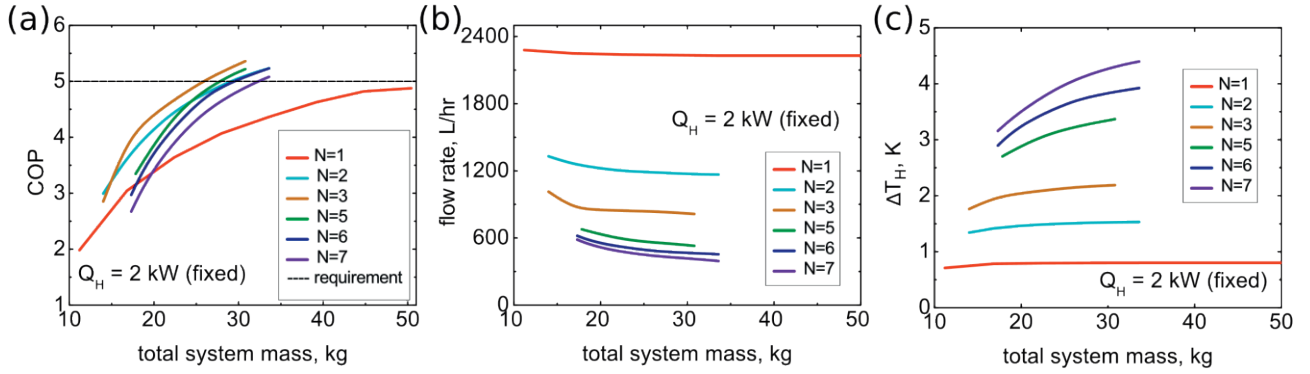


Figure 3: (a) COP_{net} , (b) m_{flow} and (c) ΔT_H vs. total magnetocaloric mass of the cascaded MCHP network

Optimization with respect to the fixed $COP_{net} = 5$ is shown in Fig. 4. It is found that the heating power curves lie close to each other and there is no optimum number of MCHPs: at smaller magnetocaloric masses, three MCHPs give larger heating power, than two, whereas for larger magnetocaloric masses the curve with $N_{HP}=2$ has higher value (dominates), signifying that the impact of heating power change in the growing network is not as critical as the impact of changing capacity. The behaviour of m_{flow} and ΔT_H has changed accordingly: their lines are more equidistant than in Fig. 3.

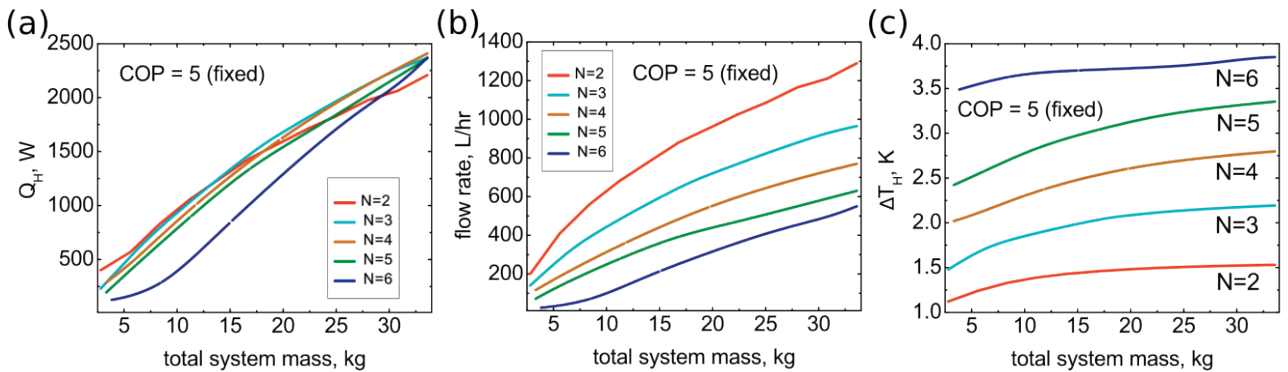


Figure 4: (a) $Q_{H,net}$, (b) m_{flow} and (c) ΔT_H vs. total magnetocaloric mass of the cascaded MCHP network

3. CONCLUSIONS

Due to fast operation of MCHPs, the small displaced volume per cycle limits their heating power. We have shown that this problem can be addressed by constructing networks with hot-to-hot and cold-to-cold connections between MCHPs. We have introduced a concept and gave a classification of magnetocaloric networks both from the point of view of their scaling and connection properties and applied this knowledge to a cascaded network with a mixed type of scaling. We have shown that

- According to calculated scaling laws, the performances of scaled and non-scaled networks are related linearly and can be automatically recalculated in lookup table-based MCHP energy models
- Magnetocaloric networks with up to 7 cascaded MCHPs have larger COPs and temperature differences across the load and require lower mass flow rate, than a single MCHP with the same magnetocaloric mass and heating power
- Magnetocaloric networks can fulfil the requirements of a residential heating system ($Q_H = 2$ kW, COP = 5)
- The optimum number of MCHP exists for networks with fixed COPs ($N_{HP} = 3$), but not for networks with fixed heating power

The main novelty of this study is the detailed presentation of a new type of magnetocaloric network with simultaneous component and system level scaling (AMR mass vs. MCHP number). It was shown that these networks can improve the performance of magnetocaloric devices. Another hypothesis which was not tested here is that due to reduced mass flow in the system, cascaded networks will require less pump power and increase the system COP, when the MCHP is connected to a borehole heat exchanger (heat source) and a residential building (heat load). Testing of this hypothesis and a more in-depth study of magnetic heating network configurations are left for future work.

NOMENCLATURE

A	AMR cross section area (cm ²)	COP	Coefficient of performance (1)
d	packed bed sphere diameter (mm)	ε	AMR porosity (1)
L	AMR length (m)	m	magnetocaloric mass (kg)
M	mass scaling factor (1)	N	number of network elements (1)
Q_H	heating power (W)	Q_C	heating capacity (W)
ρ	bulk density of the solid (kg m ⁻³)	T	temperature (K)
τ	AMR cycle period (s)	V	volume displaced during $\frac{1}{2}$ period (L hr ⁻¹)

ACKNOWLEDGEMENTS

We are grateful for financial support provided by the ENOVHEAT project funded by Innovation Fund Denmark (contract no 12-132673).

REFERENCES

- Engelbrecht, K., 2008. A Numerical Model of an Active Magnetic Regenerator Refrigerator with Experimental Validation. Ph.D. thesis, University of Wisconsin-Madison.
- Engelbrecht, K., Eriksen, D., Bahl, C.R.H., Bjørk, R., Geyti, J., Lozano, J.A., Nielsen, K.K., Saxild, F., Smith, A., Pryds, N., 2012. Experimental Results for a Novel Rotary Active Magnetic Regenerator. *Int. J. Refrigeration* 35(6), 1498-1505.
- Johra, H., Filonenko, K., Heiselberg, P., Veje, C., Lei, T., Dall'Olio S., Engelbrecht, K., Bahl, C., 2018. Integration of a magnetocaloric heat pump in a low-energy residential building. *Build. Simul.* 11(4), 753-763.
- Lei, T., Engelbrecht, K., Nielsen, K. K., Veje, C. T., 2017. Study of geometries of active magnetic regenerators for room temperature magnetocaloric refrigeration. *App. Therm. Eng.* 111, 1232-1243.
- Tahavori, M., Filonenko, K., Veje, C. T., Lei, T., Engelbrecht, K., Bahl, C., 2017. A Cascading Model Of An Active Magnetic Regenerator System. *Proceedings of the 7th International Conference on Magnetic Refrigeration at Room Temperature*, Turin, Italy, IIF/IIR, 248-251.